JOURNAL OF CATALYSIS 87, 482–496 (1984)

Nature and Properties of a Potassium-Promoted $NiMo/Al_2O_3$ Water Gas Shift Catalyst

M. KANTSCHEWA,[1] F. DELANNAY,* H. JEZIOROWSKI,[2] E. DELGADO, S. EDER, G. ERTL, AND H. KNÖZINGER[3]

*Institut für Physikalische Chemie, Universität München, Sophienstrasse 11, 8000 München 2, West-Germany and *Groupe de Physico-Chimie Minérale et de Catalyse, Université Catholique de Louvain, 1348 Louvain-la-Neuve, Belgium*

Received October 20, 1983; revised January 10, 1984

A comparative study has been performed of a conventional $NiMo/Al_2O_3$ catalyst and of this same material after impregnation with K_2CO_3. The catalysts were characterized by conventional and microprobe Raman spectroscopy, diffuse reflectance and X-ray photoelectron spectroscopy, analytical electron microscopy and temperature-programmed decomposition. The chemisorption of carbon monoxide was studied by transmission infrared spectroscopy. The results indicate a very strong interaction of K^+ ions with the catalyst surface. The original octahedral coordination of Mo^{6+} in the $NiMo/Al_2O_3$ catalyst is transformed into a tetrahedral coordination and the reducibility of Mo^{6+} is strongly decreased in the presence of K^+ ions. Also the degree of sulfidation seems to be reduced in $KNiMo/Al_2O_3$, this phenomenon being accompanied by a stabilization of the Mo^{5+} oxidation state. CO chemisorption leads to the formation of carbonates and formates on both catalysts in their oxidized and sulfided states. On reduced $KNiMo/Al_2O_3$ CO polymer anions also seem to be formed. The effect of K^+ ions on the catalytic performance of the $NiMo/Al_2O_3$ catalysts was tested for thiophene hydrodesulfurization (HDS), ethylene hydrogenation, CO methanation, and water gas shift (WGS). A significant reduction in activity was observed for HDS in the presence of K^+ ions, while the activity for WGS was simultaneously enhanced. An attempt is made to correlate the changes of the catalytic performance with the changes which are induced by K_2CO_3 impregnation on structure, symmetry, and valence state of the molybdenum species.

INTRODUCTION

Not only can molybdenum-based catalysts be used as methanation (*1*) and Fischer-Tropsch catalysts (*2*), they also play an important role as water gas shift (WGS) catalysts (*3*). This reaction is of considerable importance when the synthesis gas is derived from coal because it provides the extra hydrogen needed for CO hydrogenation since coal-derived synthesis gas has usually H_2/CO ratios less than 1. Moreover, synthesis gas frequently contains sulfur-compounds as impurities. Therefore, supported metal catalysts would require a severe sulfur clean-up whereas molybdenum-based catalysts are known to be much more sulfur-resistant. Hou *et al.* (*4*) have recently studied the kinetics of the WGS reaction on a conventional molybdena–alumina catalyst. These authors proposed a mechanism which involved a redox cycle with Mo^{5+} as an important species in WGS catalysis.

It is also known that alkali additives have a promoting effect on the WGS activity of molybdenum-based catalysts (*5, 6*). Potassium turned out to be one of the best promoters giving the most active $CoMo/Al_2O_3$ WGS catalyst (*5*) and K_2CO_3 seems to be the most recommendable potassium source for catalyst preparation (*6*).

Although $CoMo/Al_2O_3$ and $NiMo/Al_2O_3$ catalysts have been characterized extensively by various physical techniques (*7,*

[1] Permanent address: Institute of General and Inorganic Chemistry, Bulgarian Academy of Sciences, Sofia 1113, Bulgaria.

[2] Present address: WIM, 8058 Erding, FRG.

[3] To whom all correspondence should be addressed.

0021-9517/84 $3.00

8), detailed structural information of the more complex alkali-promoted systems is still lacking. Ramaswamy *et al.* (*9*) have shown that sodium enhanced the reducibility of cobalt and of molybdenum in $CoMo/Al_2O_3$ catalysts. Metallic cobalt could be detected after H_2 reduction at 770 K in the presence of sodium whereas reduction to the metal was suppressed in samples not containing sodium. Lycourghiotis *et al.* (*10*) have recently reported on the effect of Li^+ on the catalytic properties of a $CoMo/Al_2O_3$ catalyst. In this case the γ-Al_2O_3 support was modified with Li^+ cations prior to impregnation of the molybdenum and cobalt salts. A marked decrease of the catalytic activity for hydrodesulfurization (HDS) of thiophene was observed with increasing Li^+ content. The authors explain their results on the basis of the so-called bilayer model (*8, 11*) for the oxide precursor state of the catalyst and in the frame of Delmon's synergy-by-contact model (*11, 12*) for the sulfided catalysts. In continuation of this work, Kordulis *et al.* (*13*) have studied the effect of nitrates of the alkali metals (Li through Cs) on the symmetry and valence of molybdenum species formed on a γ-Al_2O_3 surface. The salient result of this study was that all modifiers inhibited the reduction of Mo^{6+} to Mo^{5+} and this effect increased with the size of the additive cation and with its concentration. All alkali cations except Li^+ produced a transition from octahedral to tetrahedral coordination of the Mo^{6+} species. The magnitude of this effect increased with increasing alkali content, but the effect was independent of the molybdate loading.

We report here on the structural characteristics of a potassium-containing $NiMo/Al_2O_3$ catalyst which was prepared by K_2CO_3 impregnation of a conventional $NiMo/Al_2O_3$ catalyst. The structural characterization was performed by means of various spectroscopic techniques and analytical electron microscopy. We also report on CO chemisorption experiments and catalytic activity measurements for the HDS of thiophene, the methanation and WGS-reaction, and for ethylene hydrogenation. Attempts will be made to correlate the differences of the catalytic performance of a $NiMo/Al_2O_3$ and a $KNiMo/Al_2O_3$ catalyst with the differences of their structural characteristics.

EXPERIMENTAL

Catalyst preparation. A $NiMo/Al_2O_3$ catalyst containing 3.5 wt% NiO and 10 wt% MoO_3 was obtained by double impregnation (pore filling method) of a γ-Al_2O_3 support (PURAL SB from CONDEA, S_{BET} = 210 m^2g^{-1}) with $Ni(NO_3)_2$ and $(NH_4)_6Mo_7O_{24}$ solutions and drying at 390 K followed by calcination at 770 K in air for 2 h after each impregnation step. The preparation procedure was the same as described previously (*14, 15*). This catalyst had a BET surface area of 184 m^2g^{-1}. Finally, this same material was impregnated with a K_2CO_3 solution and dried at 380 K. The K_2CO_3 content of the catalyst was 12 wt%, its surface area was 127 m^2g^{-1}. The atomic ratio Mo/K in this catalyst is 0.4. This material will be designated $KNiMo/Al_2O_3$ in the following.

Methods. Transmission infrared spectroscopy, temperature-programmed decomposition, and X-ray photoelectron spectroscopy were used in exactly the same way as described recently for the study of K_2CO_3/Al_2O_3 (*16*). Conventional Raman and diffuse reflectance (DRS) spectroscopies were also described previously (*14, 15*). In addition, a Raman microprobe MOLE was used to obtain spatially resolved (~1 μm) Raman spectra. The 514.5-nm line of a SPECTRA PHYSICS Ar^+ ion laser Model 165 was used for excitation. The catalyst powder was pressed to obtain small wafers which were placed into the Raman microscope.

Analytical electron microscopy was performed on a JEOL 100 CX TEMSCAN microscope with a KEVEX X-ray spectrometer. The powder samples for electron microscopy were ground in a mortar and deposited on a carbon film after dispersion

TABLE 1

Conversion Data (mol %) for Thiophene HDS, Ethylene Hydrogenation, Carbon Monoxide Methanation, and Water Gas Shift over Reduced and Sulfided $NiMo/Al_2O_3$ and $KNiMo/Al_2O_3$ at 670 K

Catalyst state	Catalyst			
	$NiMo/Al_2O_3$		$KNiMo/Al_2O_3$	
	Reduced[a]	Sulfided[b]	Reduced[a]	Sulfided[b]
Thiophene HDS[c]	—	27.1	—	12.0
Ethylene hydrogenation[d]	100	100	22.0	7.1
CO-methanation[e]	57.1	12.1	0	0
Water gas shift[f]	45.0	1.8	73.0	3.0

[a] Reduction conditions: flowing H_2 (1 bar, 50 cm^3 (min g)$^{-1}$), 670 K, 16 h.

[b] Sulfidation conditions: flowing H_2 with 1% H_2S (1 bar, 50 cm^3 (min g)$^{-1}$), 670 K, 2 h.

[c] Reaction conditions: pressure 1 bar, H_2/thiophene molar ratio = 6.5, LHSV = 3.1 g (h g_{cat})$^{-1}$.

[d] Reaction conditions: pressure 1 bar, 9.1% C_2H_4, 90.9% H_2, H_2/C_2H_4 molar ratio = 10, HSV = 3930 h^{-1}.

[e] Reaction conditions: pressure 1 bar, 14% CO, 86% H_2, H_2/CO molar ratio = 6.14, HSV = 3930 h^{-1}.

[f] Reaction conditions: pressure 1 bar, 27% CO, 73% H_2, H_2O/CO molar ratio = 1.06. HSV = 3930 h^{-1}.

in ethanol. Dispersion in water was also performed for control of the possible effect of the dispersion medium. Compounds which are soluble in water but not in ethanol should be observed only on the grids prepared by dispersion in ethanol. The micrographs obtained were indistinguishable for both dispersion media.

The catalytic tests were performed in a quartz microreactor which was applied in the continuous flow mode. Typically 1 g of catalyst was used, the particle size being in the range of 0.02 to 0.04 cm. The detailed catalyst pretreatment and reaction conditions will be summarized in Table 1, together with the conversion data.

RESULTS AND DISCUSSION

A. Physical Characterization

1. Dried state of the catalyst. A conventional $NiMo/Al_2O_3$ catalyst of the given composition (molybdena loading close to the theoretical monolayer capacity) in its oxide state after calcination at 770 K is structurally characterized by a surface polymolybdate layer in which Mo^{6+} ions occupy octahedral sites (*14, 15, 17*). A certain fraction of the Ni^{2+} promoter ions is incorporated in octahedral sites in this surface polymolybdate layer, while the remainder of the Ni^{2+} ions penetrate into the support matrix where they form a surface spinel phase (*14, 15, 17*). The surface heteropolymolybdate must be considered as the oxide precursor phase of the active sulfided NiMoS phase (*18*) of hydrotreating catalysts.

A Raman band at 950 cm^{-1} (Fig. 1, spectrum a) is characteristic for the surface heteropolymolybdate. This band is assigned as the terminal Mo=O stretching mode of the edge-sharing MoO_6-octahedra of the polymolybdate structure (*14, 19, 20*). Charge-transfer (CT) transitions in Mo–O–Mo bridges in this structure give rise to a typical strong band at 300 nm in the diffuse reflectance spectra of these catalysts (*15*) as shown in Fig. 2a. The shoulder on the

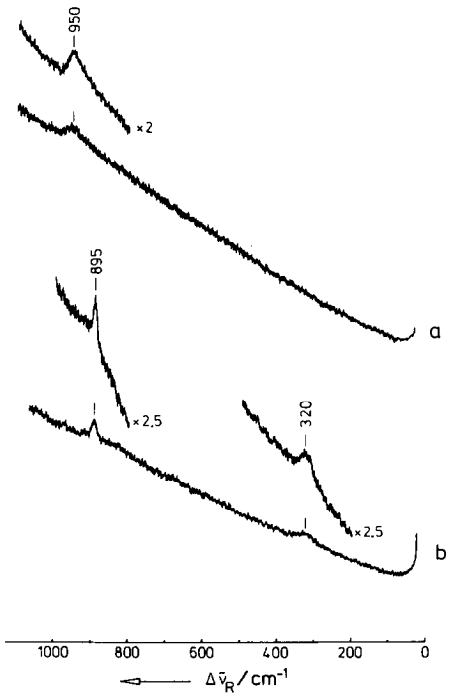

FIG. 1. Raman spectra of (a) $NiMo/Al_2O_3$ and of (b) $KNiMo/Al_2O_3$ after thermal treatment at 380 K.

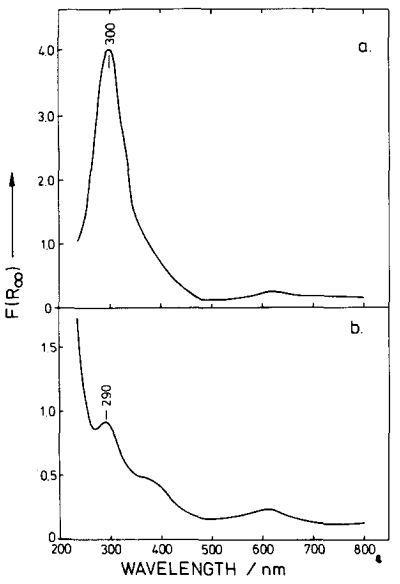

FIG. 2. Diffuse reflectance spectra of (a) $NiMo/Al_2O_3$ and of (b) $KNiMo/Al_2O_3$ after thermal treatment at 380 K.

long wavelength flank of this band between 350 and 400 nm is due to *d–d* transitions of octahedrally coordinated Ni^{2+} ions (*15*).

The impregnation with K_2CO_3 leads to dramatic changes in the Raman and optical spectra after the samples have experienced a mild heat treatment at 380 K in air. The Raman spectrum of the $KNiMo/Al_2O_3$ catalyst shows a sharp band at 895 cm^{-1} and a relatively weak broader band at 320 cm^{-1}, whereas the band at 950 cm^{-1} has essentially vanished (Fig. 1, spectrum b). This spectrum is characteristic of monomeric undistorted MoO_4^{2-} ions in which Mo^{6+} is tetrahedrally coordinated (*19*). Hence, the presence of potassium has completely destroyed the original polymolybdate surface phase and has led to a change from an octahedral coordination of Mo^{6+} to a tetrahedral coordination. This conclusion is confirmed by the diffuse reflectance spectra in the uv-region (Fig. 2b). The intense CT band at 300 nm has disappeared, only a relatively weak band at 290 nm can be observed. The absorption rises steeply below 250 nm where MoO_4^{2-} tetrahedral anions typically absorb (*19*). The destruction of the polymolybdate species of an unpromoted Mo/Al_2O_3 catalyst on addition of K_2CO_3 (Mo/K atomic ratio 0.5) has also been observed recently by TDPAC (γ-γ' time differential perturbed angular correlation), a technique which measures hyperfine interaction parameters (*40*). The Mo/K atomic ratio of 0.4 which is close to the stoichiometry in K_2MoO_4 could suggest that this compound supported on Al_2O_3 was formed although there is no direct experimental evidence for this interpretation.

The $KNiMo/Al_2O_3$ catalyst has also been studied by analytical electron microscopy after drying at 380 K. As in the case of the unpromoted $NiMo/Al_2O_3$ catalysts, careful high magnification imaging did not provide evidence of the presence (within the microporosity of the alumina grains) of a separate phase that could be distinguished from γ-Al_2O_3. X-Ray microanalysis revealed the presence of a homogeneous distribution of Ni, Mo, and K on the support. The concentration of all elements was in fair agreement with the overall composition of the samples. This confirms the Raman and DRS results, indicating that K_2CO_3 has reacted with the previously deposited nickel and molybdenum species so as to form a new type of layer covering the alumina surface.

However, in some instances a separate phase could be observed besides the γ-Al_2O_3 grains. As shown in the bright-field micrograph of Fig. 3, this phase had usually the form of thin transparent particles that can be distinguished from the darker γ-Al_2O_3 grains. It is seen that these particles are completely outside the microporosity of the support. X-Ray microanalysis showed this phase to contain only Mo and K. As mentioned above, the composition of the alumina grains did not deviate significantly from the overall catalyst composition. This suggests that only a small fraction of the total molybdenum is contained in this separate phase. (Its abundance in the micrograph of Fig. 3 is overemphasized for demonstration purposes.) The Mo/K atomic

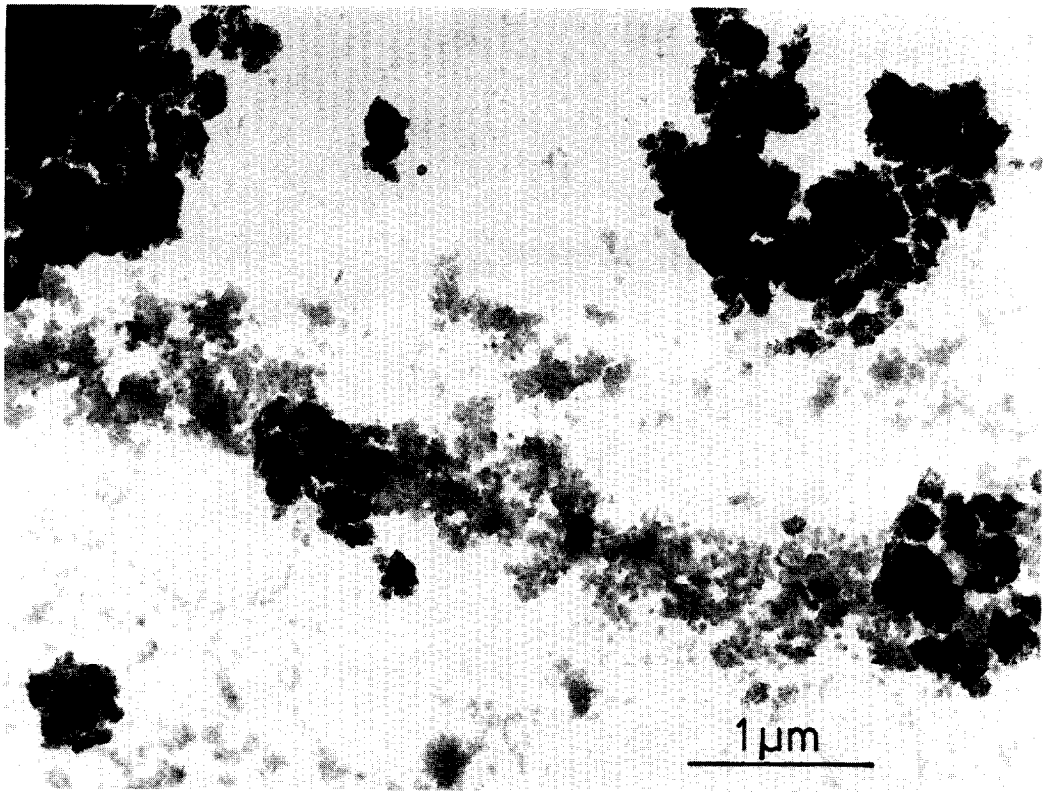

FIG. 3. Bright field electron micrograph of $KNiMo/Al_2O_3$ after thermal treatment at 380 K.

ratio in the separate phase could not be determined with very high precision from the X-ray spectra due to a lack of precise calibration of the respective sensitivities. The Mo/K atomic ratio may be estimated to be approximately 1.0 to 1.5. The relative intensities of the Mo_L and $K_{\alpha,\beta}$ lines in the X-ray spectra could vary slightly (±30%) depending on the analyzed area. The particles of this separate phase appeared to be quite crystalline (see Fig. 3). Clear ring patterns were usually obtained by electron diffraction. Exceptionally, beautiful quasi-single crystal patterns could be observed for selected particles. An example is shown in Fig. 4. This indicates the formation of an oriented layer with hexagonal symmetry.

It is clear from the observed Mo/K atomic ratio that the separate phase cannot be K_2MoO_4. Moreover, K_2MoO_4 is very soluble in water but insoluble in ethanol. K_2MoO_4 should thus have been leached out when preparing by water dispersion. As no difference was observed for the two modes of preparation, this phase is probably fairly insoluble both in water and ethanol. An unequivocal determination of the chemical identity of the separate phase is not possible at present. Among a variety of potassium molybdenum compounds, the hydrate $K_6Mo_7O_{24} \cdot 4H_2O$ is perhaps the most probable. Its Mo/K atomic ratio is in fair agreement with that found experimentally and its structure (which is unfortunately not very well established, ASTM Card 27-1367) is the most compatible with the observed diffraction pattern. In addition, potassium polymolybdate hydrates seem to have low solubility in water (CRC Handbook of Chemistry and Physics (1978), p. B-153). Such a compound may thus have precipitated during the K_2CO_3 impregnation step.

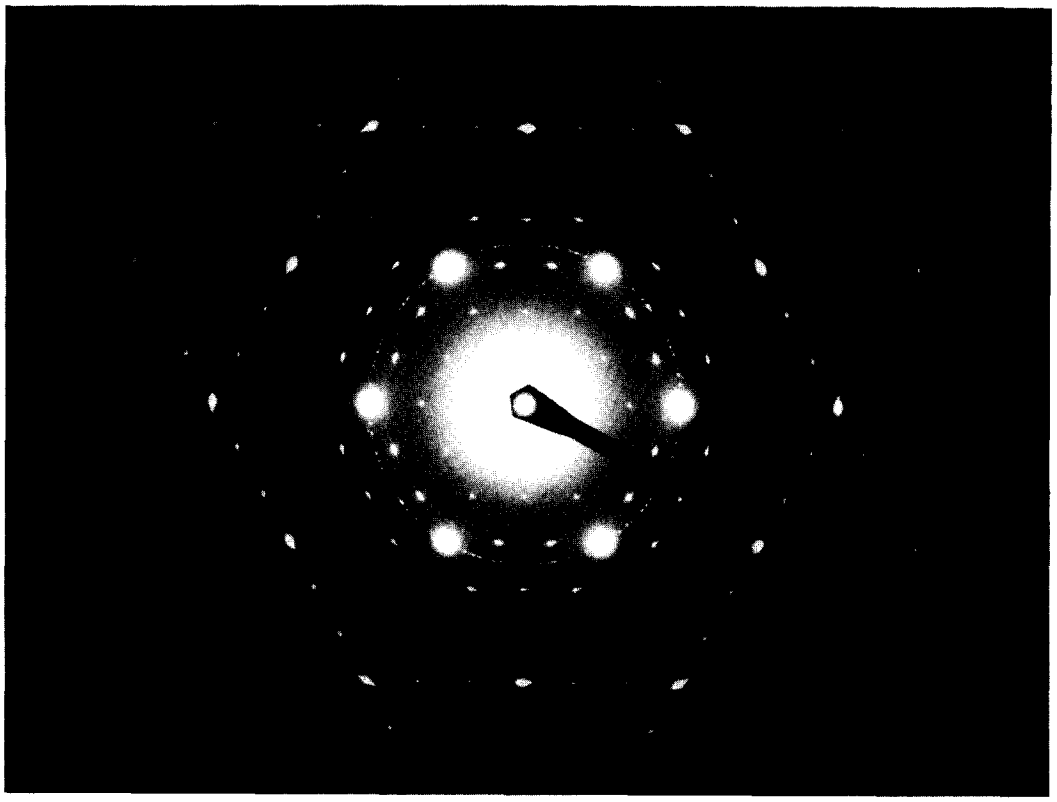

FIG. 4. Electron diffraction pattern of selected particle of the detached phase of $KNiMo/Al_2O_3$ after thermal treatment at 380 K.

The heptamolybdate anion in this compound should give rise to the typical Raman spectra of polyanions and in particular to a strong band near 950 cm^{-1}. However, the $KNiMo/Al_2O_3$ sample exclusively showed the bands of the tetrahedral monomeric MoO_4^{2-}-species (Fig. 1, spectrum b). This apparent discrepancy is due to the comparably low abundance of the separate phase in the catalyst sample. It was in fact possible to detect small particles by the Raman microprobe which are characterized by a Mo = O symmetric stretching mode at 960 cm^{-1}. An example is shown in Fig. 5. Most of the catalyst material gives spectrum A, which is typical for the monomeric tetrahedral species (bands at 325 and 890 cm^{-1}). The broad band at 835 cm^{-1} is mainly caused by the glass optics of the microscope. Spectrum B is typical for small selected particles. It still contains the bands of the monomeric species, which is due to the limited lateral resolution of about 1μm. However, a band at 960 cm^{-1} can clearly be detected in spectrum B which can be attributed to the $Mo_7O_{24}^{6-}$ anion.

The experimental results described above suggest, that the incorporation of K_2CO_3 into a $NiMo/Al_2O_3$ catalyst and mild heat treatment at 380 K leads to a complete destruction of the original polymolybdate surface phase. Mo^{6+} is coordinated tetrahedrally in the presence of K_2CO_3. A certain though relatively small portion of the surface molybdate is completely detached from the support surface and forms a separate crystalline phase, presumably $K_6Mo_7O_{24} \cdot 4H_2O$.

2. Thermal decomposition. Melting of K_2CO_3 above 1170 K was not observed in the $KNiMo/Al_2O_3$ catalyst by DTA. This supports the above observation that potas-

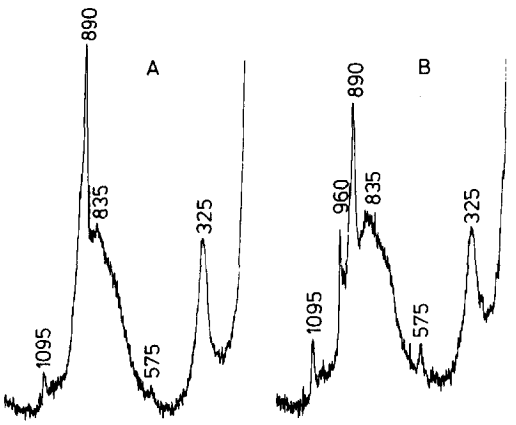

FIG. 5. Raman microprobe spectra of two selected areas of $KNiMo/Al_2O_3$ after thermal treatment at 380 K.

sium interacts strongly with the catalyst surface and is most probably not present in the form of the bulk compound K_2CO_3. This is consistent with the observed infrared spectra which are entirely different from those of bulk K_2CO_3.

During a temperature-programmed decomposition in helium of the $KNiMo/Al_2O_3$ sample (thermally pretreated at 380 K) CO_2 evolution was observed. The rate of CO_2 evolution was markedly increased in the temperature range between 470 and 600 K, giving rise to a peak maximum at 545 K as shown in Fig. 6. Water was also evolved in the entire temperature range. The decomposition profile is very similar to that reported recently for a sample containing 12 wt% K_2CO_3 only supported on alumina (*16*). It was concluded that AlOK groups were most probably formed with some K^+

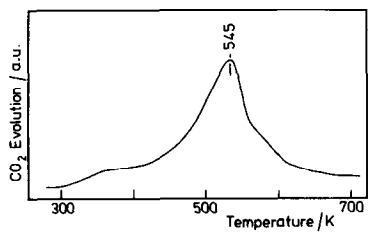

FIG. 6. Temperature-programmed decomposition in He of $KNiMo/Al_2O_3$: CO_2 evolution as a function of temperature (heating rate: 15 K min^{-1}).

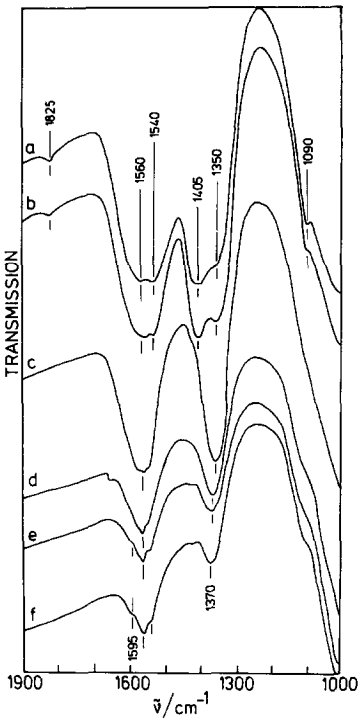

FIG. 7. Infrared transmission spectra of $KNiMo/Al_2O_3$ during thermal decomposition. Spectra taken after evacuation for 2 h at (a) 470 K; (b) 520 K; (c) 570 K; (d) 620 K; (e) 670 K; and (f) 720 K.

ions being incorporated in subsurface layers of the Al_2O_3 support. Carbonate ions were found to be coordinated to K^+ sites in mono- and bidentate form, the latter being preferred at higher temperatures. We conclude from the similarity of the behavior of the two systems during thermal decomposition that a strong interaction between potassium and the support surface must also occur in the more complex $KNiMo/Al_2O_3$ catalyst.

The transmission ir spectra in the carbonate stretching region are also very similar for the two catalysts during thermal decomposition. Figure 7 shows a series of spectra for treatment temperatures in the range between 470 and 720 K. Spectra a and b suggest the existence of mono- and bidentate carbonate species which—following the arguments in Ref. (*16*)—should most probably be coordinated to K^+ sites. Interestingly, the most significant changes in the

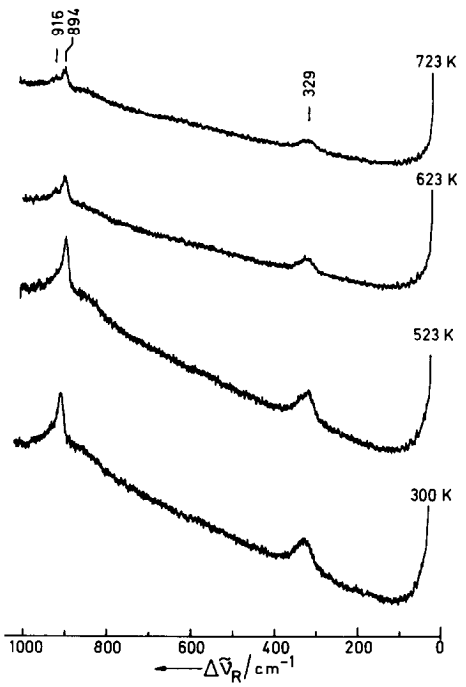

FIG. 8. Raman spectra of $KNiMo/Al_2O_3$ after thermal treatment in air at the indicated temperatures.

carbonyl infrared spectra occur in the temperature range between 520 (spectrum b) and 620 K (spectrum d) in which the sample strongly evolves CO_2. After thermal decomposition at 570 K (spectrum c) two bands are observed at 1350 and 1560 cm^{-1} which are characteristic for a bidentate carbonate coordinated to potassium (*16*). The band at 1560 cm^{-1} seems to be composite. This may indicate the presence of several carbonate species having different degrees of distortion and/or being coordinated to nonequivalent sites. After treatment at 620 K and higher temperatures when no further CO_2 evolution is observed in Fig. 6, the spectra do not change significantly any more. The bands at 1370 and 1560 cm^{-1} (with a shoulder around 1545 cm^{-1}) indicate the existence of a fairly stable bidentate carbonate species. In parallel some formate species are formed at these higher temperatures which are indicated by the appearance of the shoulder at 1595 cm^{-1}. These should also be coordinated to K^+ sites (*16*).

The molybdate species in the $KNiMo/Al_2O_3$ remain tetrahedral during these thermal treatments. This is clearly shown by the (conventional) Raman spectra of Fig. 8. At temperatures up to 520 K the characteristic Mo = O stretching mode of the "free" tetrahedral MoO_4^{2-} anion is clearly observed. This band has a slight asymmetry on its flank toward higher wavenumbers. After treatment at 620 and 720 K a second band at 916 cm^{-1} can be resolved, which must be assigned as the Mo = O stretching mode of a MoO_4^{2-} species in which the tetrahedral symmetry is distorted. This distortion will lead to a rehybridization and strengthening of terminal Mo = O bonds, and consequently to a shift of the Mo = O stretching mode to higher wavenumbers.

The chemical composition of the separate phase which was detached from the support surface after K_2CO_3 impregnation and drying at 380 K, remained unchanged during thermal decomposition as evidenced by the X-ray spectra. However, it lost its crystallinity after thermal treatment at 520 K as indicated by the glassy appearance in the electron micrograph of Fig. 9 and the complete absence of clear electron diffraction rings. This loss of crystallinity is probably connected with the loss of water from the proposed hydrate $K_6Mo_7O_{24} \cdot 4H_2O$.

3. Carbon monoxide chemisorption. CO chemisorption on *oxidized* $KNiMo/Al_2O_3$ samples was performed after their thermal decomposition at 720 K. The typical background spectrum in the ir carbonate region after this thermal treatment corresponds to spectrum f in Fig. 7. After exposure to CO pressures of 33 mbar at room temperature a weak band is observed at 2175 cm^{-1}, whereas a second weak band at 1920 cm^{-1} only becomes detectable at higher CO pressures near 395 mbar. Both bands readily vanish upon evacuation at room temperature. These two bands are assigned as carbonyl stretching modes of CO coordinated to Ni^{2+} sites (*21*) and to zero-valent Ni (*22*), respectively. The presence of the Ni^{2+} sites on the surface of the oxidized KNiMo/

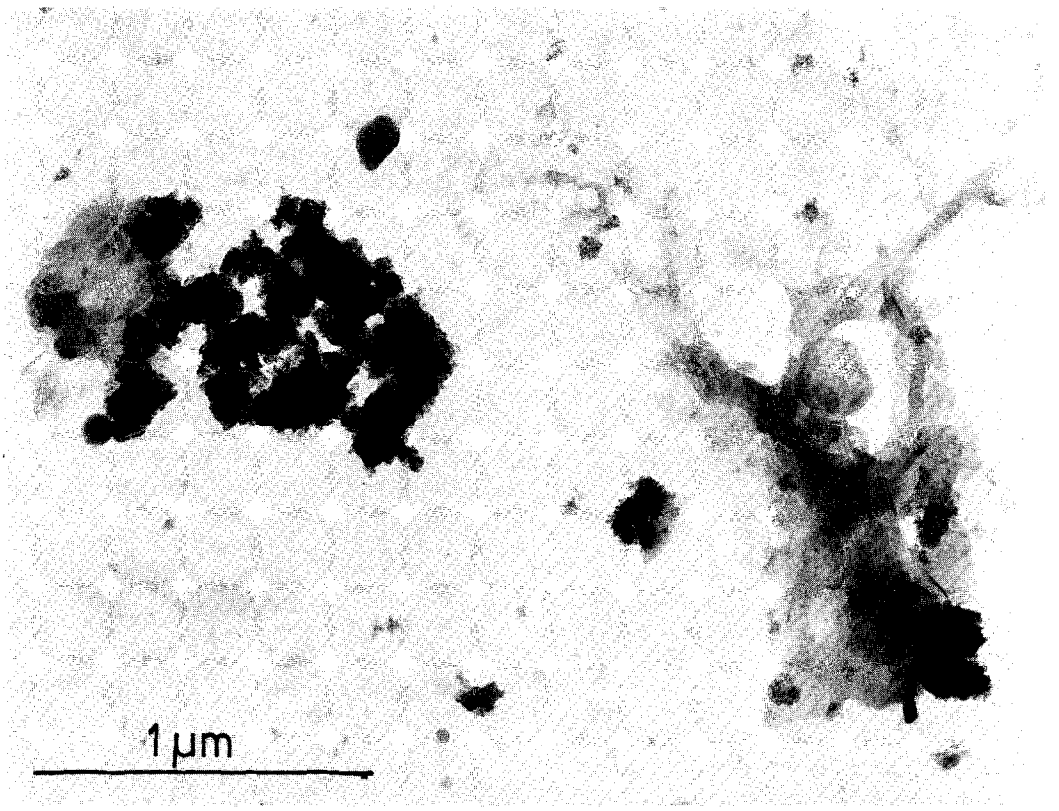

FIG. 9. Bright field electron micrograph of $KNiMo/Al_3O_3$ after thermal decomposition in air at 520 K.

Al_2O_3 catalyst is certainly not surprising. The observation of zero-valent Ni, however, is unexpected, although supported by XPS as shown in Fig. 10, where a peak at a binding energy of 853 eV also suggests the presence of Ni^0 (*23*) after thermal decomposition besides Ni^{2+} (E_b = 856.5 eV for Ni $2p_{3/2}$ (*23*)). Ni^0 must be formed during the thermal decomposition of the $KNiMo/Al_2O_3$ catalyst by a yet unknown mechanism. It can only be speculated that potassium carbonate should be involved in this reduction process. It should be mentioned in this connection that Tracy (*24*) succeeded in removing oxygen from Ni single crystal surfaces by K^+ sputtering. A very strong interaction of potassium with oxygen and joint thermal desorption was also observed on Fe surfaces by Prigge (*25*). Moreover, a weak CO and O_2 evolution was also observed during thermal decomposition and hence, some reduction of surface species should have occurred.

CO chemisorption at ir beam temperature also led to spectral changes in the carbonate/carboxylate region. The background

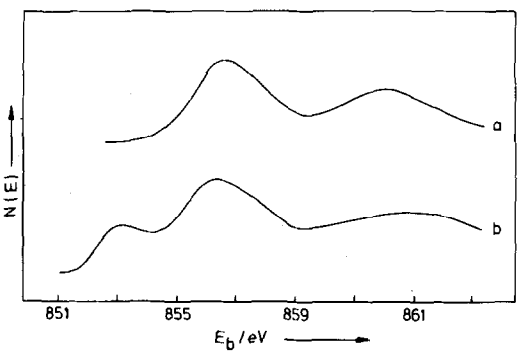

FIG. 10. Ni 2*p* photoelectron spectra of (a) $NiMo/Al_2O_3$ and of (b) $KNiMo/Al_2O_3$ after thermal treatment at 670 K.

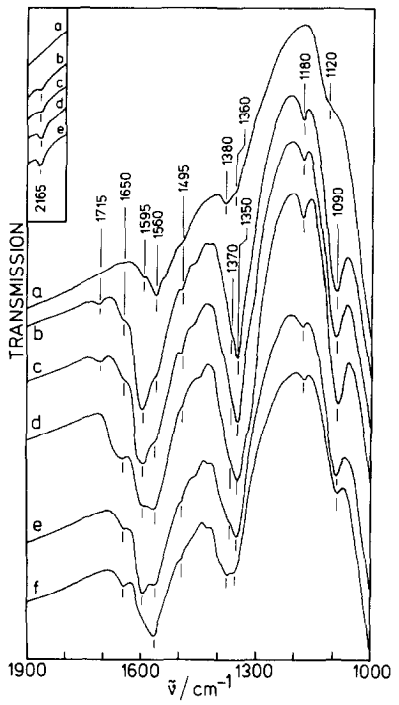

FIG. 11. Infrared transmission spectra of reduced $KNiMo/Al_2O_3$ after CO adsorption: (a) background spectrum; (b) after exposure to 263 mbar CO for 15 min at 510 K; (c) at 560 K; (d) at 620 K (samples were evacuated at 300 K for 1 h prior to recording the spectra); (e) after evacuation at 560 K for 1 h; (f) after evacuation at 620 K for 1 h.

band at 1370 cm^{-1} is significantly enhanced and a very broad band develops between 1550 and 1700 cm^{-1}. This latter band has some features which are centered at 1560, 1600, and 1650 cm^{-1}. These bands may be attributed to bidentate carbonate (1560 cm^{-1}) and carboxylate (1600 and possibly 1650 cm^{-1}) species (*16*, *26*). The species giving rise to the 1650-cm^{-1} band is rather unstable and can be pumped off at temperatures below 370 K. Evacuation at 570 K leads to an ir spectrum which is dominated by bands at 1360 and 1560 cm^{-1}. These bands are characteristic for bidentate carbonate ions which are coordinated to K^+ sites (*16*) (see also Fig. 7) and resemble very closely those observed previously on CO adsorption on K_2CO_3/Al_2O_3 (*16*).

In separate experiments, CO was adsorbed at a pressure of 263 mbar for 15 min at different temperatures. Characteristic bands are observed at 2785, 2690, 1595, and 1350 cm^{-1} which are to be assigned as the normal modes of a formate ion which is coordinated to K^+ sites (*16*, *26*). The intensities of these bands grow with temperature and pass through a maximum near 570 K. At higher temperatures, the formate seems to become thermally unstable and the exclusive species detected after CO adsorption at 670 K is the bidentate carbonate coordinated to K^+ sites (typical bands at 1570 and 1350 cm^{-1}). This behavior of the $KNiMo/Al_2O_3$ catalyst is again very similar to that reported recently for the K_2CO_3/Al_2O_3 system (*16*).

The ir spectra obtained during CO adsorption on *H_2-reduced $KNiMo/Al_2O_3$* catalysts are by far more complex than those of the oxidized form. Reduction of the catalyst was performed *in situ* in the ir cell at 620 K at an H_2 pressure of 263 mbar for 2 h followed by evacuation for 15 min. This procedure was repeated four times prior to final evacuation and CO adsorption studies. Spectrum a in Fig. 11 is the background spectrum of the reduced sample. It shows relatively weak bands of surface formate (1595 and 1360 cm^{-1}) and carbonate (1560 and 1380 cm^{-1}) species and is very similar to spectrum f in Fig. 7 of the oxidized catalyst after thermal decomposition.

CO adsorption at beam temperature produces bands in the carbonyl stretching region at 2060 and 1965–1960 cm^{-1}, which can be removed by evacuation. These bands are indicative of CO being adsorbed on zero-valent Ni particles (*22*).

At higher temperatures ($\leq$620 K) a weak band is observed at 2165 cm^{-1} (see inset in Fig. 11) indicating a thermally very stable species. The assignment of this band is not clear, although one is led to suggest some type of a CO species coordinated to a cation site (*22*). The coordination site can probably not be a Mo^{4+} site since carbonyl bands on reduced molybdena/alumina catalysts were observed at higher frequency (2195 cm^{-1}), and CO coordinated to Mo^{4+} is

much less thermally resistant (*27, 28*). Moreover, reduction of Mo under the rather mild conditions chosen here is hardly expected to occur.

As shown in Fig. 11, bands developing under a CO pressure of 263 mbar at 1715, 1650, 1595, 1560, 1495, 1370, 1350, 1180, and 1090 cm^{-1} in the carbonate/carboxylate region. In addition two bands are observed at 2780 and 2690 cm^{-1}.

The set of bands at 2780, 2690, 1595, and 1350 cm^{-1} must be assigned as the normal modes of a formate species which is coordinated to K^+ sites (*16, 26*). These bands develop already at beam temperature on the reduced $KNiMo/Al_2O_3$ catalyst, and their intensity passes through a maximum near 570 K. This behavior is very similar to that of the formate species observed on the oxidized form of the catalyst. The formate species decomposes on evacuation at temperatures above 600 K (spectrum f in Fig. 11). The band at 1650 cm^{-1} may possibly indicate the formation of a second formate species in a different environment (*26*).

A bidentate carbonate species, which is thermally rather stable, gives rise to the characteristic bands (*16*) at 1560 and 1370 cm^{-1}. These bands are the most intense bands after evacuation at temperatures above 600 K (spectrum f in Fig. 11).

The band at 1715 cm^{-1} which is observed after CO adsorption at 510 and 560 K (spectra b and c in Fig. 11) may suggest the formation of a bridged "organic-like" carbonate (*26*). This species is decomposed at higher temperatures.

The remaining bands at 1495, 1180, and 1090 cm^{-1} cannot be due to carbonate and carboxylate species. Bands at these positions are not found on the oxidized form of $KNiMo/Al_2O_3$ nor on K_2CO_3/Al_2O_3. By comparison with ir spectra reported by Guglielminotti *et al.* (*30*) for CO adsorption on alkali earth oxides, we tentatively attribute the bands at 1495, 1180, and 1090 cm^{-1} to negatively charged CO polymers. These authors had observed bands at 1480, 1275, 1197, and 1066 cm^{-1} on MgO, which they assigned as normal modes of $(CO)_n^{x-}$ or $(C_nO_{n+1})^{x-}$ where $n \geq 2$ and $x = 2,4,\ldots$

4. *Reduced and sulfided $KNiMo/Al_2O_3$.* Since this type of molybdenum-based water gas shift catalyst is known to be sulfur-resistant (*5, 6*), some XPS and ir experiments on reduced and sulfided $KNiMo/Al_2O_3$ have also been performed. Sulfidation was carried out *in situ* in an H_2/H_2S mixture (66 mbar H_2 and 6.6 mbar H_2S) for 1 h. The sulfidation temperature was 670 and 620 K, respectively, in the XPS reaction chamber and the ir cell. The samples were evacuated at the sulfidation temperature for 1 h after the H_2/H_2S treatment.

Figure 12 shows the Mo 3*d* XP spectra of the oxidized form of $KNiMo/Al_2O_3$ and of the reduced and sulfided state of this catalyst. For comparison, the XP spectra of unpromoted $NiMo/Al_2O_3$ (containing 3 wt% NiO and 12 wt% MoO_3) in the two states are also shown. The binding energies E_b

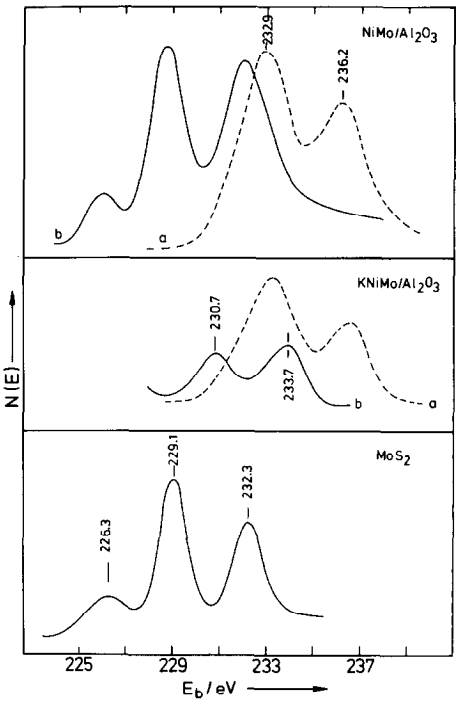

FIG. 12. Mo 3*d* photoelectron spectra of $NiMo/Al_2O_3$ and $KNiMo/Al_2O_3$ in their oxidized (calcined at 770 K in air) form (a) and in the reduced and sulfided state (b), and of MoS_2.

were evaluated using a value of 119.5 eV for the Al 2*s* level as a reference. The Mo $3d_{3/2}$ binding energies thus found for the two catalysts in the oxidized state correspond to the E_b values of Mo^{6+} as reported in the literature (*15, 31–35*), namely (236 ± 0.3) eV and (233 ± 0.3) eV, respectively, for the $3d_{3/2}$ and $3d_{5/2}$ levels.

The Mo 3*d* doublet of $NiMo/Al_2O_3$ is clearly shifted toward lower binding energies after sulfidation and the E_b values of 232.1 and 228.8 eV suggest reduction of molybdenum to Mo^{4+} (*15, 31–35*). In fact, the Mo 3*d* binding energies of MoS_2 were found to be 232.1 and 228.9 eV (*35, 36*) (see also Fig. 12) and, hence, are identical to those obtained for the reduced and sulfided $NiMo/Al_2O_3$ catalyst. The integrated intensity ratio of the $3d_{3/2}$ and $3d_{5/2}$ peaks is approximately 0.7 in the oxidized state. This value corresponds to the theoretical intensity ratio as given by Scofield (*37*) and is equal to that found for the MoS_2 reference compound (Fig. 12). This intensity ratio is found to be closer to 1 for the reduced and sulfided $NiMo/Al_2O_3$ catalyst. It is therefore concluded that some Mo^{5+} species should be present in the catalyst after sulfidation, the majority oxidation state of Mo, however, is +4. Oxidation states lower than +4 cannot be detected; the peak at 226.1 eV is due to emission from the S 2*s* level.

In contrast, reduction and sulfidation of the $KNiMo/Al_2O_3$ produces a Mo 3*d* doublet at 233.7 and 230.7 eV. These values are very close to those reported in the literature (*31, 33, 34*) for Mo^{5+}. Since the integral intensity ratio of these two peaks is larger than unity, one must assume that even Mo^{6+} is still present in the catalyst. The presence of potassium in the catalyst obviously decreases the reducibility of the molybdate, and prevents the formation of a MoS_2-like surface species. This behavior may be related to the fact that K_2CO_3 impregnation destroys the surface polymolybdate structure with Mo in octahedral coordination and leads to the formation of tetrahedrally coordinated Mo species. It was in fact reported that tetrahedral Mo is less susceptible to reduction and sulfidation than octahedral Mo (*38*).

These observations are supported by CO adsorption on the reduced and sulfided catalysts. Exposure of an unpromoted $NiMo/Al_2O_3$ catalyst to CO after reduction and sulfidation produced an infrared carbonyl stretching band at 2190 cm^{-1} which is assigned to CO coordinated to Mo^{4+} sites (*27, 28*). No such band could be observed after identical sulfidation treatment on $KNiMo/Al_2O_3$. The absence of this band is in agreement with the lower degree of reduction of this catalyst as shown by XPS.

It is interesting to note that during CO adsorption on the sulfided $KNiMo/Al_2O_3$ catalyst bands developed at 1595 and 1350 cm^{-1} even at beam temperature which conclusively confirm the formation of formate species. Since these species are considered as intermediates of the water gas shift reaction (*16, 39*), their observation is in agreement with the activity of the sulfided $KNiMo/Al_2O_3$ for this reaction. It is also interesting to recall that Hou *et al.* (*4*) have recently suggested a redox cycle with Mo^{5+} as an important species in WGS catalysis on Mo/Al_2O_3 catalysts.

B. Catalytic Performance

Steady state conversions for thiophene HDS, C_2H_4 hydrogenation, CO methanation, and WGS at 1 bar pressure and 670 K are summarized in Table 1, where the catalytic performance of $NiMo/Al_2O_3$ and $KNiMo/Al_2O_3$ is compared in the reduced and pre-sulfided states of the catalysts. The chosen standard reaction conditions are given in the footnote of Table 1.

HDS activity is reduced significantly in the presence of potassium in the catalyst. This inhibiting effect of potassium can be related to the fact that K^+ led to a change of the Mo coordination from octahedral to tetrahedral in the oxide precursor state and to the pronounced decrease in reducibility.

This decreased degree of reduction should also lead to a decreased degree of sulfidation in the K-containing catalyst. We infer that as a consequence the active NiMoS phase (*18*) cannot be sufficiently developed in the K-containing catalysts which then must necessarily lead to a decrease of HDS activity.

Stationary conversions for C_2H_4 hydrogenation were 100% both on the reduced and on the sulfided $NiMo/Al_2O_3$ catalyst at the chosen high temperature of 670 K. However, potassium had a very strong inhibiting effect and led to conversions of only 22 and 7.1% for the reduced and the sulfided $KNiMo/Al_2O_3$ catalyst, respectively, under identical reaction conditions.

The CO methanation reaction on $NiMo/Al_2O_3$ is poisoned by sulfur. However, the catalyst remains active in its sulfided form. In contrast, $KNiMo/Al_2O_3$ is absolutely inactive under the applied reaction conditions for the methanation reaction both in its reduced and sulfided state.

As shown in Table 1, the activity for the WGS reaction is very significantly enhanced when K_2CO_3 is introduced in the $NiMo/Al_2O_3$ catalyst. This activity increase may be due to either of two effects or to a cooperation of both. First, the formation of formate species during adsorption of CO is strongly enhanced by K^+ ions. Therefore, the stationary concentration of a possible formate intermediate (*16, 39*) may be increased. Second, the Mo^{5+} oxidation state seems to be stabilized in the presence of K^+ ions in the catalyst. Following the discussion of Hou *et al.* (*4*) for a Mo/Al_2O_3 catalyst, the Mo^{5+} species may play an important role in a redox mechanism of the WGS reaction also on the catalyst system studied here. The data presented in Table 1 also show that the $NiMo/Al_2O_3$ catalyst is strongly poisoned by presulfidation, and this is also true for the $KNiMo/Al_2O_3$ catalyst. Nevertheless, the activity of the K-containing catalyst is still higher by a factor of about 2 than that of $NiMo/Al_2O_3$ in the sulfided state.

C. Effect of Varying Potassium Contents

The effect of varying potassium contents (<12 wt% K_2CO_3) was tested in a few preliminary experiments. In contrast to $KNi Mo/Al_2O_3$ containing 12 wt% K_2CO_3 (Mo/K atomic ratio = 0.4), catalysts having lower K_2CO_3 contents (4 wt%) show Raman spectra which are characteristic of the simultaneous presence of polymolybdate and monomeric MoO_4^{2-}-species. The same conclusion could be drawn from γ-γ' time differential perturbed angular correlation (TDPAC) measurements (*40*) on an unpromoted Mo/Al_2O_3 catalyst after addition of 6 wt% K_2CO_3 (Mo/K atomic ratio = 0.8). These results suggest that there is a gradual destruction of the initially present polymolybdate phase as K_2CO_3 is added to the catalyst in increasing amounts up to 12 wt% K_2CO_3. The formation of a stoichiometric compound such as K_2MoO_4 can neither be directly detected nor excluded.

The gradual destruction of the polymolybdate species is also reflected in the trends of catalytic performance with increasing potassium content. Some preliminary data are summarized in Table 2 for the simultaneous WGS reaction and ethylene hydrogenation on three $NiMo/Al_2O_3$ catalysts (3.5 wt% NiO, 10 wt% MoO_3) containing 0, 4, and 8 wt% K_2CO_3, respectively. These data clearly demonstrate that the WGS activity increases with K_2CO_3 con-

TABLE 2

Conversion Data (mol %) for Simultaneous WGS and Ethylene Hydrogenation on $KNiMo/Al_2O_3$ with Varying Potassium Content[a]

K_2CO_3 content (wt%)	Conversion of CO (mol%)	Conversion of C_2H_4 (mol%)
0	23.5	~98
4	58.9	~58
8	77.2	~26

[a] Reaction conditions: 560 K, 28 bar, GHSV =4500 l (h kg_{cat})$^{-1}$. Feed gas composition: 6%, CO, 32% CO_2, 0.3% H_2S, 2% C_2H_4 in flowing H_2.

tent while simultaneously ethylene hydrogenation activity is decreasing.

CONCLUSIONS

The following conclusions can be drawn from the experimental results:

1. Potassium interacts strongly with the support surface and the molybdate phase.
2. Molybdenum is coordinated octahedrally in $NiMo/Al_2O_3$, while it is coordinated tetrahedrally in $KNiMo/Al_2O_3$.
3. Addition of K_2CO_3 destroys the surface heteropolymolybdate phase and hence, the precursor for the NiMoS active phase of a sulfided $NiMo/Al_2O_3$ catalyst.
4. As a consequence, the NiMoS phase cannot sufficiently be developed in the presence of potassium.
5. After reduction and sulfidation, the Mo^{5+} oxidation state is stabilized in $KNiMo/Al_2O_3$, while Mo^{4+} is preferred in $NiMo/Al_2O_3$.
6. The structural modifications induced by K_2CO_3 addition lead to remarkable changes of the catalytic performance.
7. Activities for thiophene HDS and ethylene hydrogenation are significantly reduced in $KNiMo/Al_2O_3$.
8. Methanation activity vanishes in the presence of potassium.
9. WGS activity is enhanced in the presence of potassium.
10. The reduced HDS activity can presumably be related to an inhibition of the NiMoS phase formation, while WGS activity may be enhanced by an increased stationary concentration of a formate intermediate and may be related to the stabilization of the Mo^{5+} oxidation state.
11. No clear conclusions regarding the relevance of Ni in these catalysts can be drawn from the present results. Additional experiments are required and in progress.

ACKNOWLEDGMENTS

This work was financially supported by the Deutsche Gesellschaft für Mineralölwissenschaft und Kohleforschung, by the Deutsche Forschungsgemeinschaft and by the Fonds der Chemischen Industrie. M. K. received a grant from the German Academic Exchange Service (DAAD). We gratefully acknowledge the assistance of Dr. K. Kochloefl and Dr. D. Prigge, Südchemie AG, Moosburg, FRG, with the catalytic tests and of Mr. Baur with the temperature-programmed decomposition experiments.

REFERENCES

1. Wilhelm, F. C., Tsigdinos, G. A., and Ferenc, R. A., *in* "Proceedings, Climax 3rd International Conference on Chemistry and Uses of Molybdenum" (H. F. Barry and P. C. H. Mitchell, Eds.), p. 219. Climax Molybdenum Co., Ann Arbor, Michigan, 1979.
2. Murchison, C. B., *in* "Proceedings, Climax 4th International Conference on Chemistry and Uses of Molybdenum" (H. F. Barry and P. C. H. Mitchell, Eds.), p. 197. Climax Molybdenum Co., Ann Arbor, Michigan, 1982.
3. Aldrige, C. L., and Kalina, T., U.S. Patent 3,850,840 (1974); Segura, M., Aldrige, C. L., Riley, K. L., and Pine, L. A., U.S. Patent 3,974,096 (1976).
4. Hou, P., Meeker, D., and Wise, H., *J. Catal.* **80,** 280 (1983).
5. Newsome, D. S., *Catal. Rev.-Sci. Eng.* **21,** 275, (1980).
6. Deflin, M., Clement, J. C., Germaine, G., and Grand, C., German OLG DE 30 42 326 A1, 1981.
7. Massoth, F. E., *Advan. Catal.–Rel. Subj.* **27,** 265 (1978).
8. Grange, P., *Catal. Rev.-Sci. Eng.* **21,** 135 (1980).
9. Ramaswamy, A. V., Sivasanker, S., and Ratnasamy, P., *J. Catal.* **42,** 107 (1976).
10. Lycourghiotis, A., Vattis, D., Karaiskakis, G., and Katsanos, N., *J. Less-Common Met.* **86,** 137 (1982).
11. Delmon, B., *in* "Proceedings, Climax 3rd International Conference on Chemistry and Uses of Molybdenum" (H. F. Barry and P. C. H. Mitchell, Eds.), p. 73. Climax Molybdenum Co., Ann Arbor, Michigan, 1979.
12. Apecetche, M. A., and Delmon, B., *React. Kinet. Catal. Lett.* **12,** 385 (1979).
13. Kordulis, C., Violotis, S., and Lycourghiotis, A., *J. Less-Common Met.* **84,** 197 (1982).
14. Knözinger, H., Jeziorowski, H., and Taglauer, E., "Proceedings, 7th International Congress on Catalysis, Tokyo, 1980, Kodansha, Tokyo," Vol. 1, 604. Elsevier, Amsterdam, 1981.
15. Abart, J., Delgado, E., Ertl, G., Jeziorowski, H., Knözinger, H., Thiele, N., Wang, X. Zh., and Taglauer, E., *Appl. Catal.* **2,** 155 (1982).
16. Kantschewa, M., Albano, E. V., Ertl, G., and Knözinger, H., *Appl. Catal.* **8,** 71 (1983).
17. Jeziorowski, H., Knözinger, H., Taglauer, E., and Vogdt, C., *J. Catal.* **80,** 286 (1983).

18. Topsøe, H., Clausen, B. S., Candia, R., Wivel, C., and Mørup, S., *Bull. Soc. Chim. Belg.* **90,** 1190 (1981).
19. Jeziorowski, H., and Knözinger, H., *J. Phys. Chem.* **83,** 1166 (1979).
20. Dufresne, P., Payen, E., Grimblot, J., and Bonnelle, J. P., *J. Phys. Chem.* **85,** 2344 (1981).
21. Borello, E., Cimino, A., Ghiotti, G., LoJacono, M., Schiavello, M., and Zecchina, A., *Discuss. Faraday Soc.* **52,** 149 (1971).
22. Sheppard, N., and Nguyen, T. T., *Advan. Infrared Raman Spectrosc.* **5,** 67 (1978).
23. Ertl, G., Hierl, R., Knözinger, H., Thiele, N., and Urbach, H. P., *Appl. Surf. Sci.* **5,** 49 (1980).
24. Tracy, J. C., *J. Chem. Phys.* **56,** 2736 (1972).
25. Prigge, D., Doctoral thesis, University of Munich, 1982.
26. Busca, G., and Lorenzelli, V., *Mater. Chem.* **7,** 89 (1982).
27. Delgado, E., Canosa Rodrigo, B., and Knözinger, H., in preparation.
28. Millman, W. S., Crespin, M., Cirillo, C., Jr., Abdo, S., and Hall, W. K., *J. Catal.* **60,** 404 (1979).
29. Guglielminotti, E., Coluccia, S., Garrone, E., Cerruti, L., and Zecchina, A., *J. Chem. Soc. Faraday I* **75,** 96 (1979).
30. Coluccia, S., Garrone, E., Guglielminotti, E., and Zecchina, A., *J. Chem. Soc. Faraday I* **77,** 1063 (1981).
31. Cimino, A., and de Angelis, B. A., *J. Catal.* **36,** 11 (1975).
32. Declerck-Grimee, R. I., Canesson, P., Friedman, R. M., and Fripiat, J. J., *J. Phys. Chem.* **82,** 885 (1978).
33. Okamoto, J., Tomiaka, H., Katoh, Y., Imanaka, T., and Teranishi, S., *J. Phys. Chem.* **84,** 1833 (1980).
34. Haber, J., Marczewski, W., Stock, J., and Ungier, L., *Ber. Bunsenges. Phys. Chem.* **79,** 970 (1975).
35. Patterson, T. A., Carver, J. C., Leyden, D. E., and Hercules, D. M., *J. Phys. Chem.* **80,** 1700 (1976).
36. Alstrup, I., Chorkendorff, I., Candia, R., Clausen, B. S., and Topsøe, H., *J. Catal.* **77,** 397 (1982).
37. Scofield, J. H., *J. Electron Spectrosc. Relat. Phenom.* **8,** 129 (1976).
38. Grimblot, J., Dufresne, P., Gengembre, L., and Bonnelle, J. P., *Bull. Soc. Chim. Belg.* **90,** 1261 (1981).
39. Amenomiya, Y., and Pleizier, G., *J. Catal.* **76,** 345 (1982).
40. Vogdt, C., Butz, T., Lerf, A., and Knözinger H., to be presented at the 8th International Congress on Catalysis, West-Berlin, 1984.